

NINETEENTH EUROPEAN ROTORCRAFT FORUM

Paper n° D10

REDUCED TIP SPEED TESTING
OF A VARIABLE DIAMETER TILTROTOR

by

David Matuska, Anthony Saccullo
SIKORSKY AIRCRAFT, USA

Karen Studebaker
NASA AMES RESEARCH CENTER, USA

September 14-16, 1993
CERNOBBIO (Como)
ITALY

ASSOCIAZIONE INDUSTRIE AEROSPAZIALI
ASSOCIAZIONE ITALIANA DI AERONAUTICA ED ASTRONAUTICA

REDUCED TIP SPEED TESTING OF A VARIABLE DIAMETER TILTROTOR

David Matuska, Anthony Saccullo

SIKORSKY AIRCRAFT
Stratford, Connecticut, USA

Karen Studebaker

NASA AMES RESEARCH CENTER
Moffett Field, California, USA

Abstract

This paper reviews the aeroelastic scaling methodology for reduced tip speed testing and documents the results from a wind tunnel test of a 1/6th scale Variable Diameter Tiltrotor (VDTR). This test was a joint effort of NASA Ames and Sikorsky Aircraft. Testing was performed at one-half of full-scale tip speed with the rotor system aeroelastically scaled for accurate dynamic response at this reduced tip speed. Reduced tip speed testing provides accurate aeroelastic results with the advantages of scaled-down power requirements and rotor loads, and also greater test safety. The objective was to evaluate the aeroelastic and performance characteristics of the VDTR in conversion, hover, and cruise. This test represents the first wind tunnel test of a variable diameter rotor applied to a tiltrotor concept. The results confirm the potential advantages of the VDTR and establish the variable diameter rotor a viable candidate for an advanced tiltrotor.

1. Introduction

Sikorsky Aircraft has been developing the Variable Diameter Tiltrotor (VDTR) concept for a number of years, and the benefits of the variable diameter concept have been discussed in previous papers (Ref. 1-3). The National Aeronautics and Space Administration (NASA) is currently conducting and sponsoring research with the goal of developing an advanced civil tiltrotor by the year 2005. Advanced proprotor technology will play a major role in the success of an advanced civil tiltrotor. The results of four studies contracted by NASA reemphasized the importance of advanced proprotor technology (Ref. 4). The current test was part of NASA's focused research effort to investigate and develop an efficient and quiet rotor for advanced civil tiltrotor aircraft. Jointly sponsored by NASA Ames and Sikorsky Aircraft, this test was conducted to confirm the feasibility and to quantify several of the benefits of the variable diameter rotor for tiltrotor aircraft.

Anticipated benefits of the variable diameter rotor for tiltrotors are numerous. The VDTR reduces the rotor design compromise between hover and cruise performance. The primary advantage of a large hover diameter is the low disk loading. This allows for reduced hover downwash, lower noise and improved takeoff and autorotative characteristics. The smaller diameter in cruise results in improved propeller efficiency, lower gust response, and reduced internal and external noise. Furthermore, the variable diameter tiltrotor can operate efficiently at a constant RPM in both hover and cruise unlike conventional tiltrotors. Figure 1 illustrates a conceptual drawing of a VDTR in both airplane and helicopter modes.

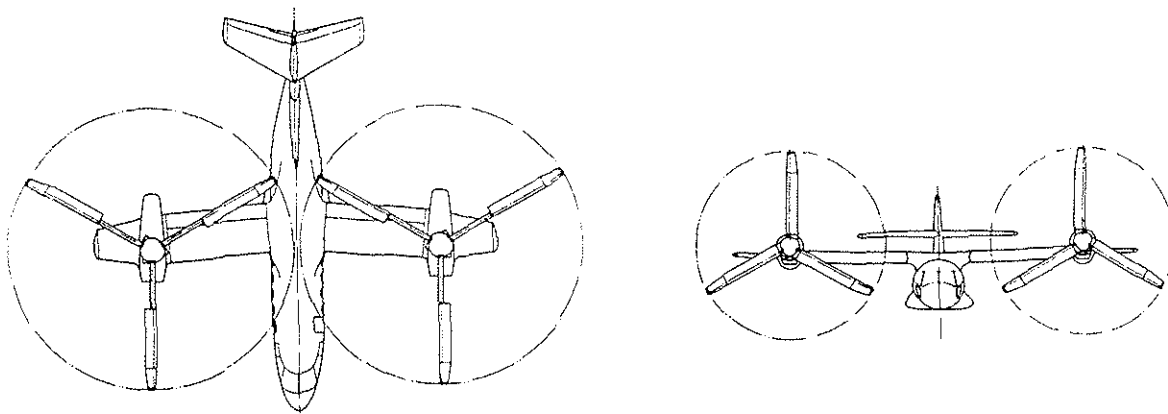


Figure 1. Conceptual VDTR Civil Tiltrotor Schematic

The wind tunnel test described here was the first such test of the variable diameter concept for a tiltrotor and successfully demonstrated the feasibility of this combination. The test utilized a 1/6th scale semi-span tiltrotor model with full remote control capability of both nacelle tilt and rotor diameter. The model was tested at the United Technologies Research Center (UTRC) 18 foot wind tunnel. The purpose of this test was to evaluate aeroelastic and performance characteristics of the variable diameter tiltrotor model in conversion, hover and cruise. In addition, stability derivatives and control power characteristics were explored. Data were acquired through a test matrix that included rotor diameter variation from 66 to 100% coordinated in discrete steps and a nacelle tilt angle variation from zero (cruise) to 90 degrees (hover). Figure 2 illustrates the model rotor capability as representative of a conceptual conversion regime. The successful results of this joint NASA and Sikorsky test have established the feasibility of the VDTR and demonstrated the advantages of the variable diameter concept.

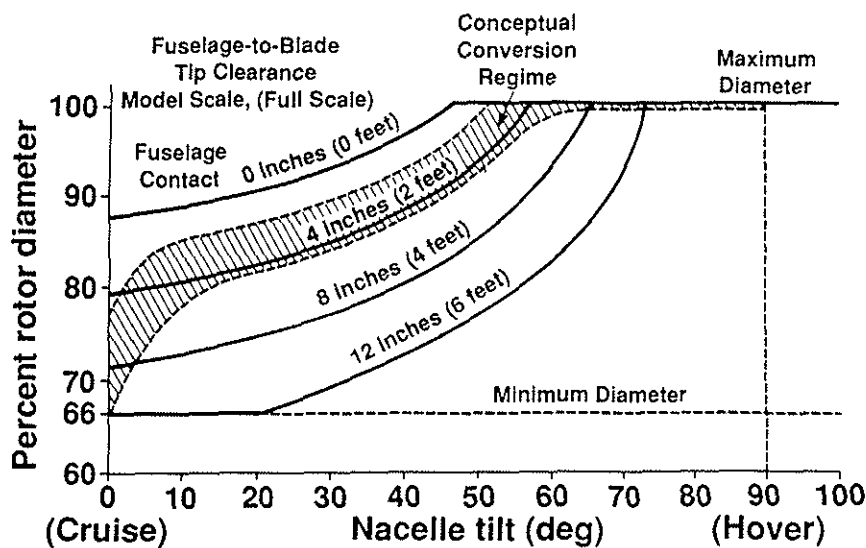


Figure 2. Rotor Diameter Range vs. Nacelle Tilt for the Variable Diameter Tiltrotor Model.

2. Reduced Tip Speed Testing

Certain laws of similarity must be observed in order to ensure that model test data can be applied for full-scale designs. Geometric similarity is necessary to ensure airflow streamline similarity between the test article and the full-scale article. There are various laws of dynamic similitude which must be adhered to, depending on the test objectives. These laws will affect the model design and construction techniques, test philosophy and data analysis.

The forces exerted on a body moving through a fluid arise from the interaction of the inertia of the body to gravity, fluid viscosity and fluid elasticity. The most common force ratios used for obtaining dynamic similarity are: 1) Reynolds Number = Inertia Force / Viscous Force; 2) Mach Number = Inertia Force / Elastic Force; and, 3) Froude Number = Inertia Force / Gravity Force. It is not necessary for all of these force ratios to remain identical between model and full-scale hardware for useful test results. However, the validity and accuracy of the test data will depend on how closely one or more of these model-scale ratios represent their full-scale counterparts. The force ratios of primary importance depend on the specific test objectives.

For rotary wing testing involving performance investigations, matching of the Mach Number is of primary importance. The Reynolds Number effects are not as critical as long as the model scale is large enough. The model should be physically sized to operate at a Reynolds Number as close as practical to the full-scale Reynolds Number. Often the model size is determined by wind tunnel size or test rig power availability. Froude Number scaling is normally ignored for performance testing since gravity forces are small and have no noticeable effect on performance.

For aeroelastic tests where the objective is dynamic stability or flutter investigation, the Froude Number is critical. Fabrication of a model which duplicates full-scale stiffness and mass while keeping Froude Number equal to one is extremely difficult. This is especially true for rotating components such as rotor blades. Froude scale rotor blades tend to be very delicate and are easily damaged with normal handling associated with model assembly and testing. Typically these blades are constructed with the blade spar producing all the required stiffness and a trailing edge pocket area that contributes aerodynamic shape with little or no stiffness contribution.

Often there is a need to acquire dynamic stability data and qualitative aerodynamic performance data from a model during the same test entry. A technique involving reduced tip speed (RTS) scaling is commonly employed at Sikorsky to meet this objective. Typically, 1/2 tip speed is selected to result in model scaling in between the Mach and Froude scaling.

There are numerous advantages to testing a RTS model since this type of model possesses the characteristics of both Mach and Froude scaling. These advantages include: 1) Accurate dynamic response data and qualitative performance data can be reliably obtained. However, the data from a model of this type needs to be carefully evaluated for Froude effects on the aeroelastic results and Reynolds effects on performance results. Froude effects for this test were assumed negligible and inconsistencies in Reynolds number between the model and full-scale produces roughly accurate performance data. 2) The power requirements to drive the rotor and to operate the control system are significantly reduced. Power required for a 1/2 tip speed test is 1/8 the power required for a similar Mach-scale test. 3) Blade construction is simplified and damage is avoided since they can be made more substantial. 4) Test safety is improved due to lower tip speed operation. Also, hardware failures are less likely to be catastrophic.

Scale factors for a variety of model parameters are presented in Table 1 for Mach, Reduced Tip Speed, and Froude scale testing, where

S = Full Scale Dimensions / Model Dimensions

u = Full Scale (Simulated) Velocities / Model Test Velocities

σ = Full Scale (Simulated) Air Density / Model Test Air Density

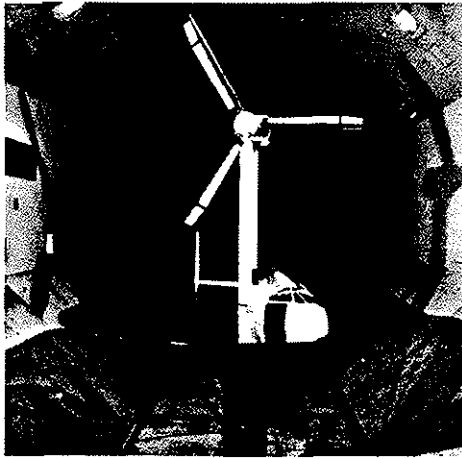
For this test, S = 6, u = 2, and σ is assumed to equal one. For proper scaling, model dimensional parameter values must be equal to full scale parameter values times the factors indicated.

Table 1 Model Scale Factors

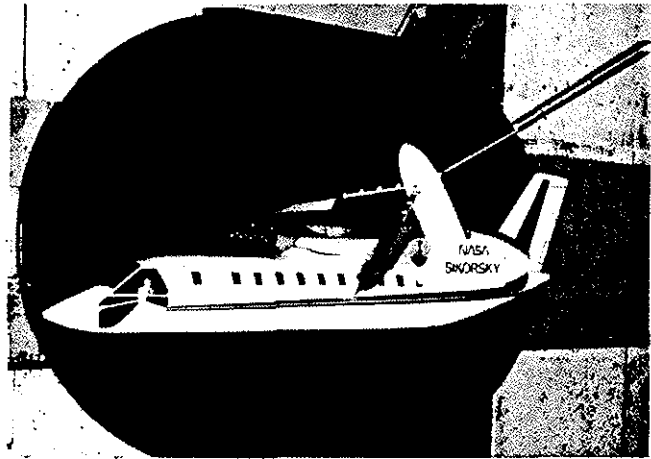
	MACH	REDUCED TIP SPEED (GENERAL)	FROUDE
ADVANCE RATIO ($v/\Omega R$)	1	1	1
ANGULAR ACCELERATION	S^2	$S^2 u^{-1}$	S
ANGULAR DISPL. - DYNAMIC	1	1	1
ANGULAR SPRING STIFFNESS	$S^{-3} \rho^{-1}$	$S^{-3} u^{-2} \rho^{-1}$	$S^{-4} \rho^{-1}$
ANGULAR VELOCITY	S	$S u^{-1}$	$S^{1/2}$
DISK LOADING	σ^{-1}	$u^{-2} \rho^{-1}$	$S^{-1} \rho^{-1}$
FORCE	$S^{-2} \rho^{-1}$	$S^{-2} u^{-2} \rho^{-1}$	$S^{-3} \rho^{-1}$
FREQUENCY	S	$S u^{-1}$	$S^{1/2}$
FROUDE NUMBER	S	$S u^{-2}$	1
LINEAR DIMENSIONS	S^{-1}	S^{-1}	S^{-1}
LINEAR DISPLACEMENT - DYNAMIC	S^{-1}	S^{-1}	S^{-1}
LINEAR SPRING STIFFNESS	$S^{-1} \rho^{-1}$	$S^{-1} u^{-2} \rho^{-1}$	$S^{-2} \rho^{-1}$
LINEAR VELOCITY	1	u^{-1}	$S^{-1/2}$
MACH NUMBER	1	u^{-1}	$S^{-1/2}$
MASS MOMENT OF INERTIA	$S^{-5} \rho^{-1}$	$S^{-5} \rho^{-1}$	$S^{-5} \rho^{-1}$
MASS OR WEIGHT	$S^{-3} \rho^{-1}$	$S^{-3} \rho^{-1}$	$S^{-3} \rho^{-1}$
MOMENT AND TORQUE	$S^{-3} \rho^{-1}$	$S^{-3} u^{-2} \rho^{-1}$	$S^{-4} \rho^{-1}$
NATURAL FREQUENCIES	S	$S u^{-1}$	$S^{1/2}$
REYNOLDS NUMBER	$S^{-1} \rho^{-1}$	$S^{-1} u^{-1} \rho^{-1}$	$S^{-3/2} \rho^{-1}$
PER REV FREQUENCIES	1	1	1
POWER	$S^{-2} \rho^{-1}$	$S^{-2} u^{-3} \rho^{-1}$	$S^{-7/2} \rho^{-1}$
STIFFNESS (EI, GJ)	$S^{-4} \rho^{-1}$	$S^{-4} u^{-2} \rho^{-1}$	$S^{-5} \rho^{-1}$
STRAIN	1	1	1
TIME (eg. for one revolution)	S^{-1}	$S^{-1} u$	$S^{-1/2}$
<p>S = Full Scale Dimensions / Model Dimensions u = Full Scale (Simulated) Vel / Model Test Vel ρ = Full Scale (Simulated) Density / Model Test Density</p> <p>For proper scaling, model dimensional parameter values must be equal to full scale parameter values times the factors indicated.</p>			

3. Model Description

The VDTR model used in this test was a 1/6th scale semi-span model installed in the tunnel so that the wing was positioned vertically and the rotor was located near the center of the tunnel cross section. The model is illustrated in a cruise configuration with the rotor fully retracted and in a conversion configuration with the rotor fully extended in Figure 3. It is aeroelastically scaled for accurate rotor dynamics and loads at one-half tip speed operation. Model operating tip speeds were 340 and 224 fps for maximum and minimum diameters, respectively. The three-bladed rotor system has a maximum extended rotor diameter of 8.2 ft and a minimum diameter of 5.4 ft which corresponds to a 34% diameter reduction.



Cruise Configuration
(Min Diameter)



Conversion Configuration
(Max Diameter)

Figure 3. Variable Diameter Tiltrotor Model.

The rotor design incorporates a jackscrew retraction/extension mechanism, which has been described in previous papers (Refs. 1-3). The model rotor utilized a reversible electric motor to actuate the jackscrew mechanism for blade extension and retraction. Figure 4 illustrates the VDTR model rotor blade. The rotor blades were of all-composite construction and utilized advanced Sikorsky airfoil sections with 31 degrees of linear twist and a tapered tip. Photographs of model blade components are presented in Figure 5.

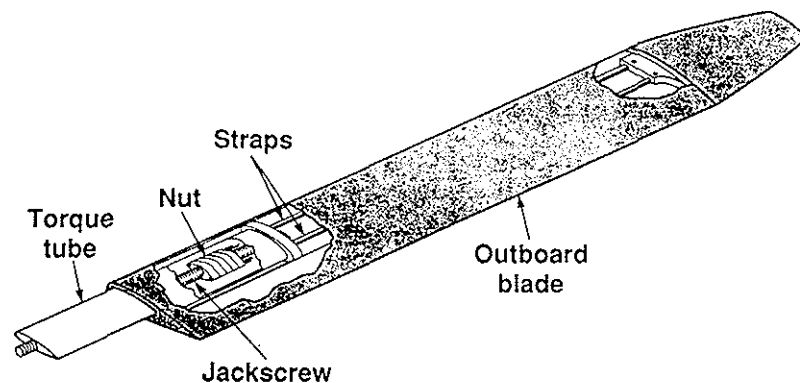


Figure 4. VDTR Model Blade Schematic

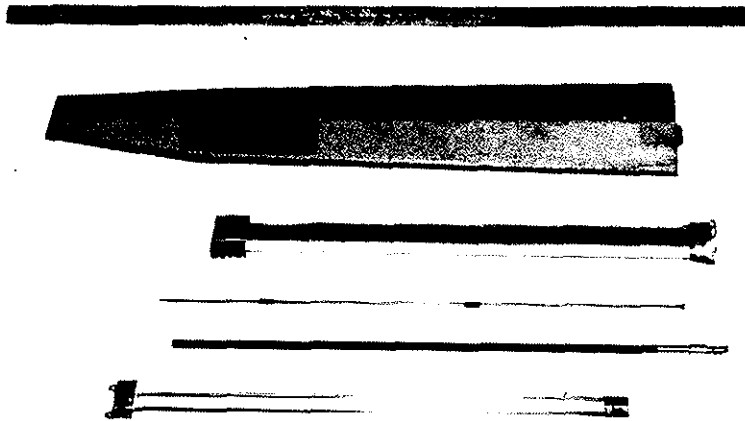


Figure 5. VDTR Model Blade Components

The model's gimballed hub is illustrated in Figure 6. Rotor torque was delivered via a mechanical link torque drive. Three links were used to provide a constant speed universal joint action for the gimbal. Twelve steel loop springs were arranged around the azimuth of the hub to provide the desired gimbal hub stiffness.

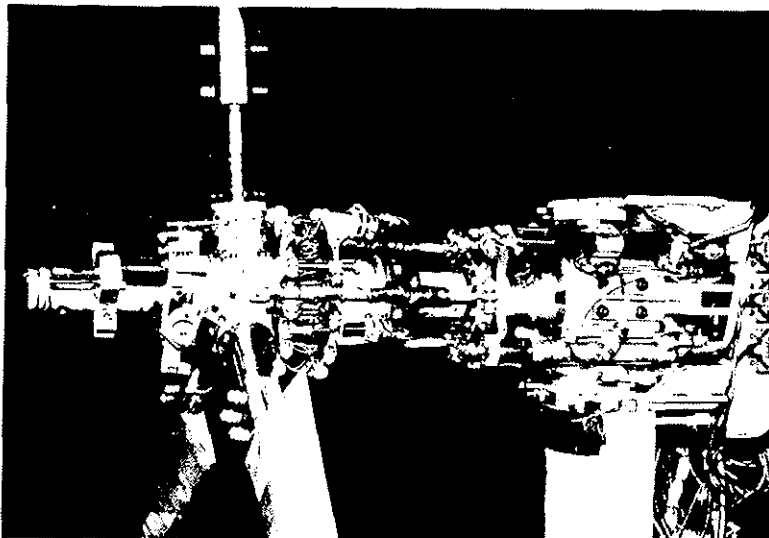


Figure 6. VDTR Model Hub Installation

The semi-span test rig (Figure 3) consisted of a rigid wing supporting a nacelle. A reflection plane was mounted on the aircraft plane of symmetry to study aerodynamic interference effects at low forward speeds. The rigid wing allowed the experimental investigation to concentrate on the dynamics and performance of the rotor alone. A half-fuselage was mounted on the ground plane as shown in Figures 3A & B.

One of the rotor blades was instrumented with fourteen strain gage bridges, including five flatwise, five edgewise, and four torsion gages. The torque tube had flatwise, edgewise and torsion gages located at 10%, 25% and 40% of maximum radius. Outboard blade strain gages included flatwise and edgewise gages located at 53% and 75% of maximum radius and a torsion gage located at 65% of maximum radius. These positions were chosen to ensure adequate definition of the radial distribution of strain.

4. Test Results and Analysis

4.a Nondimensionalization Conventions

Because the rotor diameter was a variable during this test, it was necessary to adopt certain conventions in presenting the data. The interpretation of rotor force measurements required an unconventional means of nondimensionalization because the rotor diameter varied throughout conversion. This changes the rotor solidity which is normally a constant in rotor performance coefficients. In order to directly compare rotor coefficients regardless of the rotor diameter configuration, performance data here are nondimensionalized using the fully extended values of radius and solidity. An asterisk is utilized to denote that this convention is being used. The advantage of using a common base for the data is that direct comparisons of the extended blade conditions (helicopter mode and early conversion) and retracted conditions (late conversion and cruise) may be made.

4.b Test Envelope

Significant data were acquired throughout the conversion corridor, as well as for hover and cruise. Figure 7 illustrates the range of test points acquired during this test with a plot of nacelle tilt versus equivalent full-scale airspeed. The full-scale airspeed is twice the tunnel velocity as a result of the half tip-speed scaling. Also illustrated in this figure is the demonstrated conversion corridor for both the XV-15 and the V-22 (Refs. 5, 6).

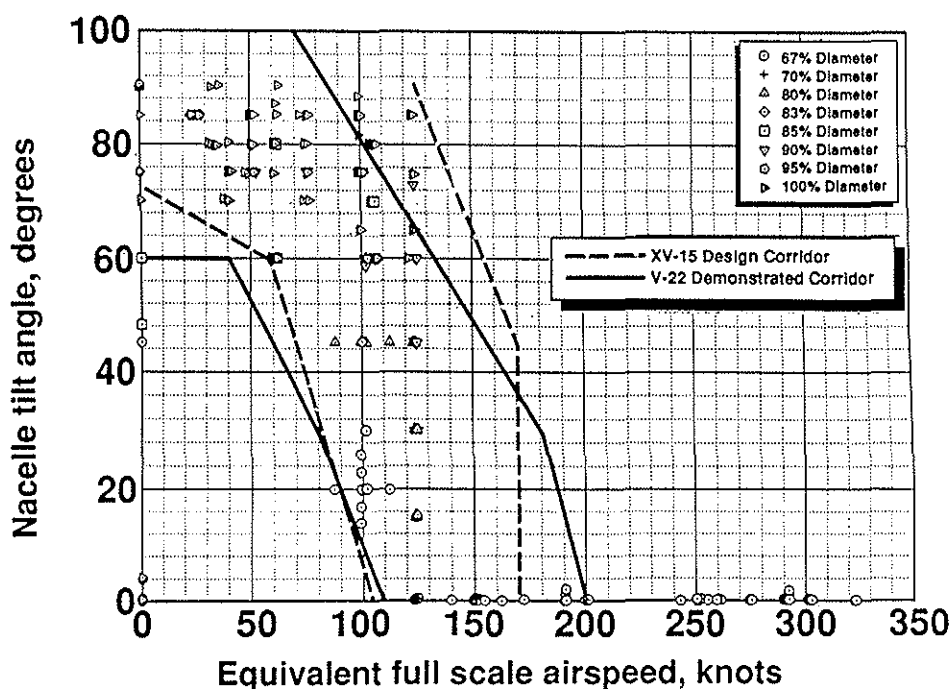


Figure 7. Range of Test Points Acquired

Figure 8 illustrates the propulsive force measured in conversion in terms of rotor C_L/σ^* versus rotor C_D/σ^* for equivalent full-scale velocities of 75, 100, 125 and 150 knots. The rotor is fully converted to the cruise configuration at 150 knots. Boundaries in the lower right of the figure illustrate the limits of C_L/σ^* and C_D/σ^* required to sustain flight in conversion for wing C_L 's ranging from 0.5 to 1.5. Test results reveal that the VDTR is capable of significantly higher propulsive force than required for conversion.

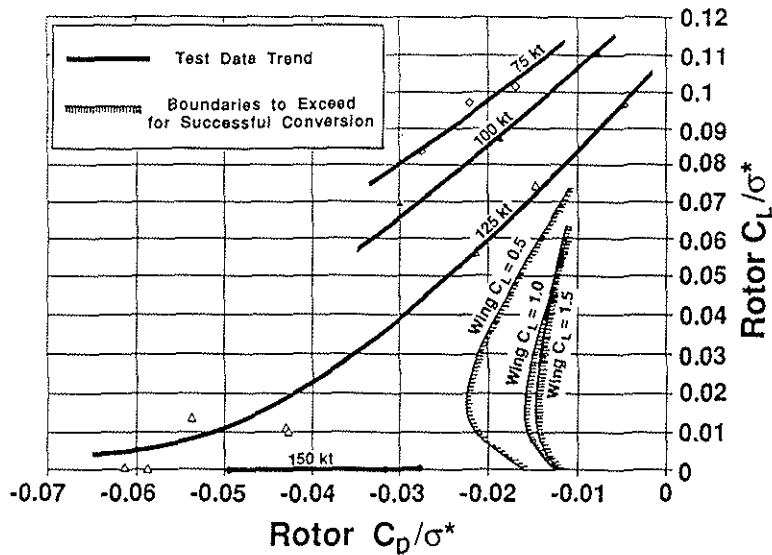


Figure 8. VDTR Propulsive Force Demonstrated Exceeds the Requirements for Successful Conversion.

4.c Blade Loads

Blade loads encountered during the course of this test are all well within the allowable loads for the VDTR blade. Aeroelastic scaling of model blade stiffnesses and loads results in the same conclusion for the full-scale design.

The full range of blade flatwise and edgewise root steady moments encountered during the test is illustrated in Figure 9. These were the worst-case blade loads encountered. The outer boundary line on this plot illustrates the ultimate strength of the blade root-end based on component testing. The inner line illustrates a moment level that is 50% of the ultimate. This lower level was chosen as a conservative limit for this test. All steady blade loads were well within the structural capability of the VDTR blade.

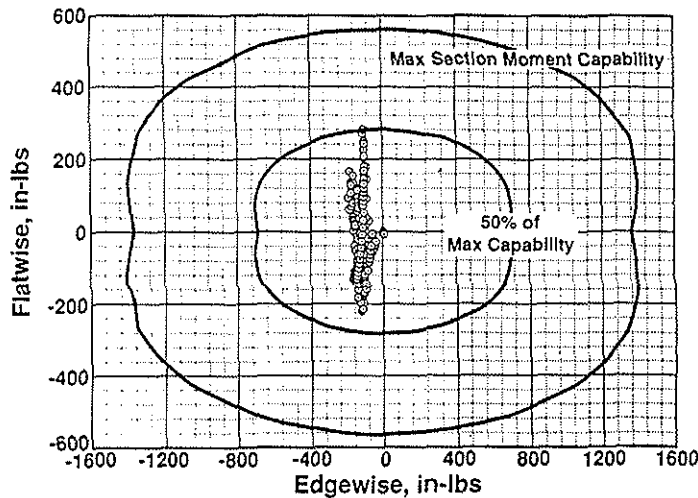


Figure 9. Measured Blade Root Steady Moments

Figure 10 illustrates the range of blade flatwise and edgewise vibratory root moments encountered. Here the outer boundary indicates the root-end section moment levels for infinite blade life based on the results of a fatigue test. The inner line indicates moment levels of half that allowed for infinite life. Again the inner boundary was used as a conservative limit for this test. As shown in the figure, this boundary limited some of the test conditions. However, all vibratory blade loads were well within the structural capability of the VDTR blade.

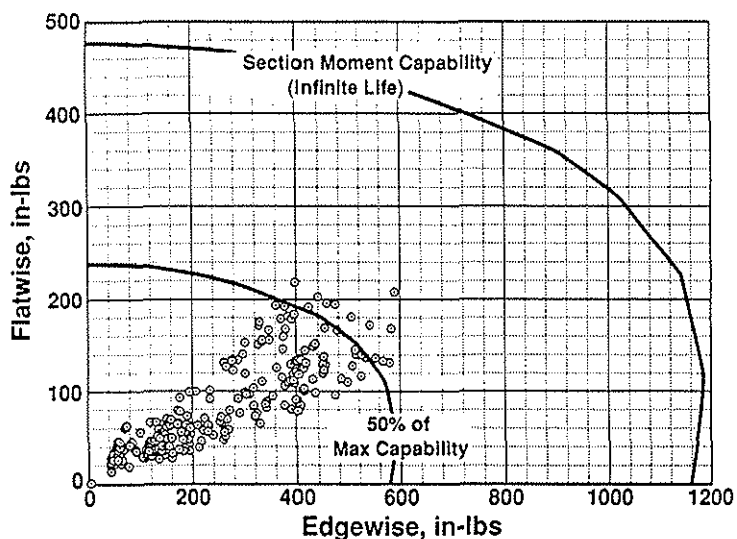


Figure 10. Measured Blade Root Vibratory Moments

Distributed blade vibratory moments for the fully extended rotor are illustrated in Figure 11 for an equivalent full-scale velocity of 106 knots and a C_t/σ^* of 0.0957. The edgewise moments are typically 2 to 3 times higher than the flatwise moments.

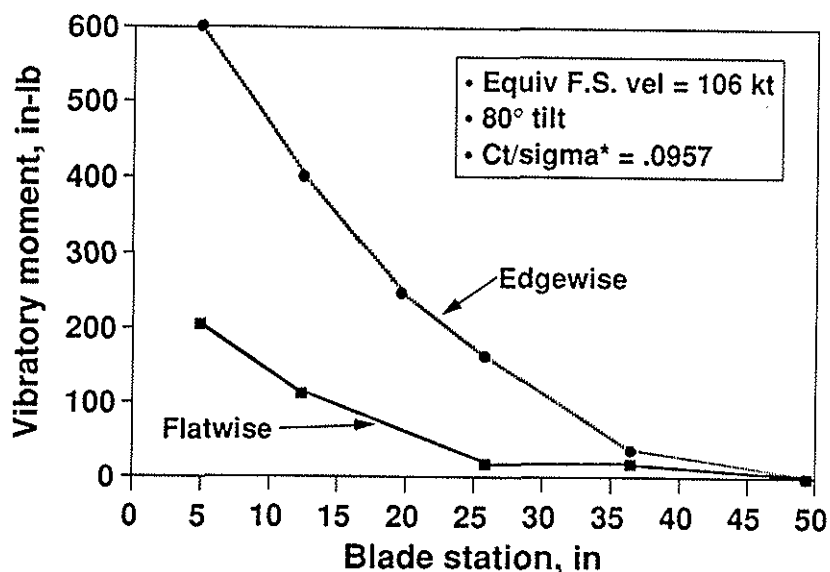


Figure 11. Distributed Vibratory Blade Moments at Maximum Diameter

Figure 12 illustrates blade moments for the rotor retracted to 85% diameter in conversion. Data is plotted separately for the torque tube and outboard blade to illustrate the overlap of the two components and to illustrate the resulting load share between these two structures. Outboard blade vibratory moments are fairly consistent for both conditions. Of significance is the fact that blade loads did not increase as the blade edgewise frequency approached and crossed 2P near this diameter configuration. In fact, diameter change was found to be very benign with no indication of blade load elevation due to frequency crossings.

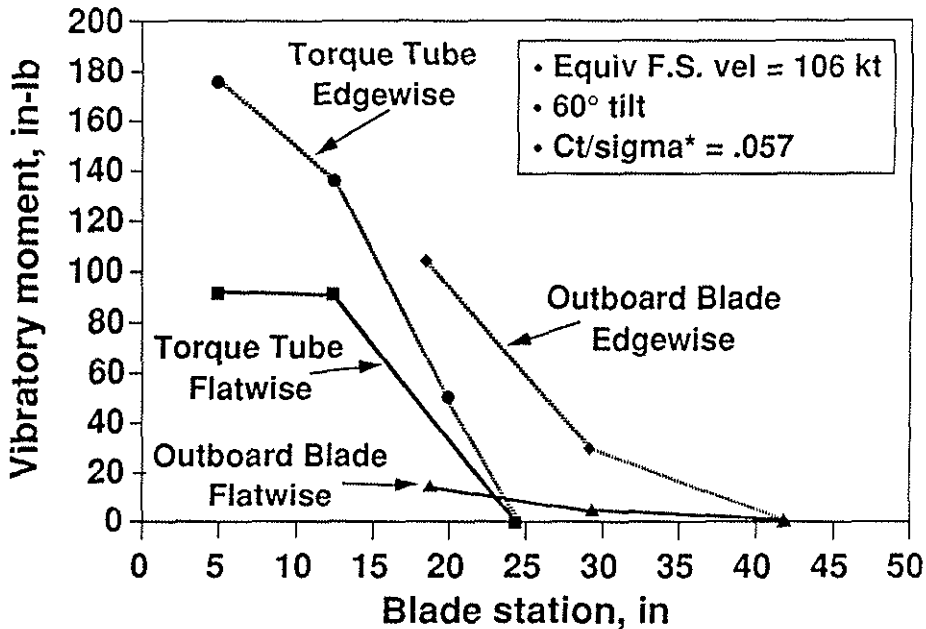


Figure 12. Distributed Vibratory Blade Moments at 85% Diameter

Blade loads continued to drop as diameter was reduced to the fully retracted configuration. Distributed moments for the fully retracted rotor are illustrated in Figure 13 for an equivalent full-scale velocity of 290 knots. Again, the torque tube and outboard blade contributions are illustrated separately. Flatwise moments increase with tunnel velocity and thrust while edgewise moments appear relatively insensitive to condition changes.

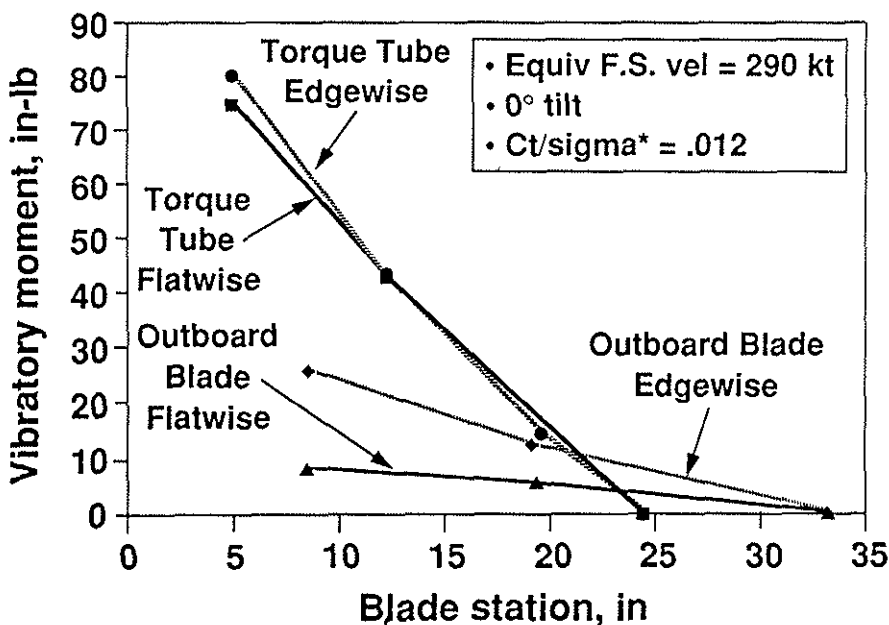


Figure 13. Distributed Vibratory Blade Moments at Minimum Diameter

4.d Cruise Performance

As illustrated in the test envelope shown in Figure 7, extensive data were acquired in the cruise conuration for equivalent full-scale velocities ranging from 150 to 325 knots. Figure 14 illustrates rotor cruise efficiency (ratio of propulsive power to shaft power) as a function of c_t/σ^* . Although this model was not Mach-scaled for accurate performance measurements, rough performance measurements were made. The cruise efficiencies calculated show good VDTR performance despite the Reynolds number inconsistencies of reduced tip speed scaling.

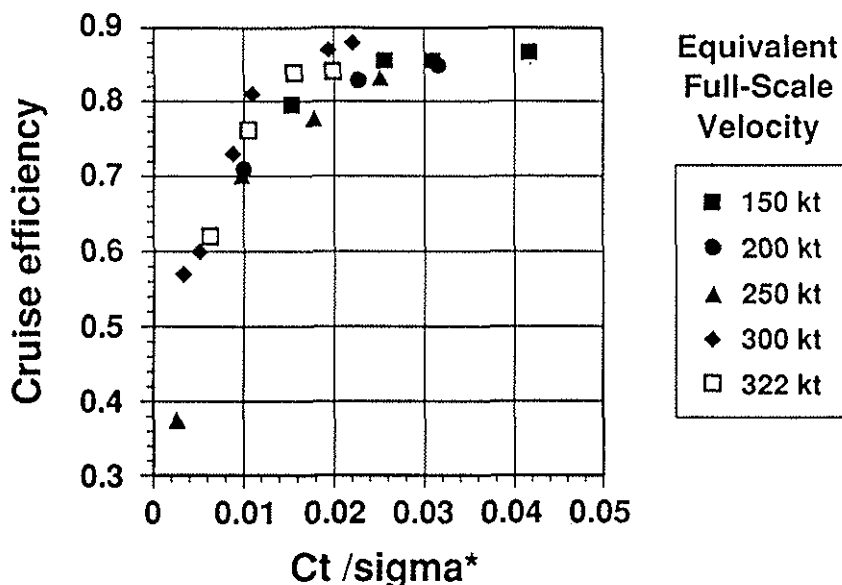


Figure 14. VDTR Cruise Performance

4.e Gust Response

An important VDTR attribute revealed during earlier studies (Ref. 3) and confirmed by this test is an impressive reduction in horizontal gust response relative to conventional tiltrotors. Gust response is a major concern in turbulent weather because the fixed diameter rotors of existing tiltrotor aircraft are oversized in cruise and thus prone to high levels of uncomfortable gust response.

Horizontal gust response was evaluated by incrementing tunnel speed by 15 fps (representing a quasi-steady 30 fps gust at full-scale) about a trim point without changing collective or cyclic pitch. Figure 15 reveals the horizontal gust loading measured during the test. The test data are compared to predicted results (Ref. 3) for both a conventional and a variable diameter tiltrotor. Correlation is good between test data and predictions for the VDTR. The significantly higher gust response for the conventional tiltrotor is attributed to increased blade area, higher tip speed, lower blade pitch angles, and lower mean lift coefficients relative to the VDTR.

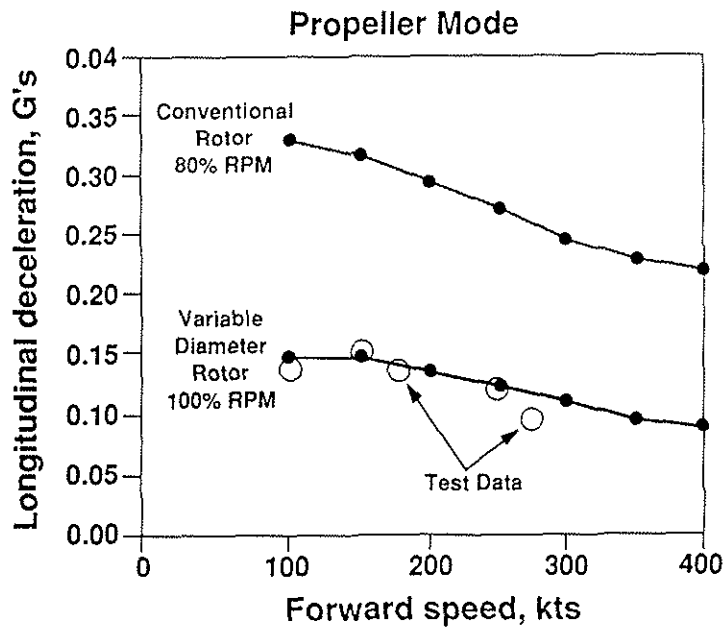


Figure 15. VDTR Simulated 30 fps Horizontal Gust Response

5. Conclusions

A 1/2 tip speed test of an aeroelastically scaled VDTR model has proven the feasibility of the variable diameter rotor for the tiltrotor application. The test has demonstrated satisfactory propulsive force and acceptable blade loads in hover, conversion and cruise with no instabilities. The VDTR concept was shown to have a number of advantages over conventional tiltrotors such as improved hover performance with lower disk loading, reduced hover downwash and significantly reduced longitudinal gust response in cruise.

6. List of References

1. Fradenburgh, E., Improving Tiltrotor Aircraft Performance with Variable-Diameter Rotors, Fourteenth European Rotorcraft Forum, Milan, Italy, Sept. 1988.
2. Fradenburgh, E., Merging Two Ends of the VSTOL Spectrum, Eighteenth European Rotorcraft Forum, Avignon, France, Sept. 1992.
3. Fradenburgh, E., and Matuska, D., Advancing Tiltrotor State-of-the-Art with Variable Diameter Rotors, American Helicopter Society 48th Annual Forum, Washington, DC, June 1992.
4. Talbot, P., High Speed Rotorcraft: Comparison of Leading Concepts and Technology Needs, American Helicopter Society 47th Annual Forum, Phoenix, AZ, May 1991.
5. Dunford, P., Lunn, K., Magnuson, R., and Marr, R., The V-22 Osprey - A Significant Flight Test Challenge, 16th European Rotorcraft Forum, Glasgow, Scotland, Sept. 1990.
6. Maisel, M., et al., Army/NASA XV-15 Tiltrotor Familiarization Document, NASA TM X-62,407, Jan. 1975.